energies

MDPI

Article

Dynamic CO_2 Leakage Risk Assessment of the First Chinese CCUS-EGR Pilot Project in the Maokou Carbonate Gas Reservoir in the Wolonghe Gas Field

Jingwen Xiao [1], Chengtao Wei [2,*], Dong Lin [1], Xiao Wu [1], Zexing Zhang [2] and Danqing Liu [2]

[1] Research Institute of Safety, Environmental Protection and Technical Supervision, PetroChina Southwest Oil & Gas Field Company, Chengdu 610041, China; xiaojingwen@petrochina.com.cn (J.X.); lin_dong@petrochina.com.cn (D.L.); wuxiao1010@petrochina.com.cn (X.W.)
[2] School of Environmental Studies, China University of Geosciences, Wuhan 430074, China; 17835033308@163.com (Z.Z.); liudq@cug.edu.cn (D.L.)
* Correspondence: chengtaowei@cug.edu.cn

Abstract

Existing CO_2 leakage risk assessment frameworks for CO_2 capture, geological storage and utilization (CCUS) projects face limitations due to subjective biases and poor adaptability to long-term scale sequestration. This study proposed a dynamic risk assessment method for CO_2 leakage based on a timeliness analysis of different leakage paths and accurate time-dependent numerical simulations, and it was applied to the first CO_2 enhanced gas recovery (CCUS-EGR) pilot project of China in the Maokou carbonate gas reservoir in the Wolonghe gas field. A 3D geological model of the Maokou gas reservoir was first developed and validated. The CO_2 leakage risk under different scenarios including wellbore failure, caprock fracturing, and new fracture activation were evaluated. The dynamic CO_2 leakage risk of the CCUS-EGR project was then quantified using the developed method and numerical simulations. The results revealed that the CO_2 leakage risk was observed to be the most pronounced when the caprock integrity was damaged by faults or geologic activities. This was followed by leakage caused by wellbore failures. However, fracture activation in the reservoir plays a neglected role in CO_2 leakage. The CO_2 leakage risk and critical risk factors dynamically change with time. In the short term (at 5 years), the project has a low risk of CO_2 leakage, and well stability and existing faults are the major risk factors. In the long term (at 30 years), special attention should be paid to the high permeable area due to its high CO_2 leakage risk. Factors affecting the spatial distribution of CO_2, such as the reservoir permeability and porosity, alternately dominate the leakage risk. This study established a method bridging gaps in the ability to accurately predict long-term CO_2 leakage risks and provides a valuable reference for the security implementation of other similar CCUS-EGR projects.

Keywords: CO_2 leakage; risk assessment; CCUS-EGR; numerical simulation; Wolonghe gas field

check for updates

Academic Editor: Alireza Nouri

Received: 25 May 2025
Revised: 5 July 2025
Accepted: 7 July 2025
Published: 22 August 2025

Citation: Xiao, J.; Wei, C.; Lin, D.; Wu, X.; Zhang, Z.; Liu, D. Dynamic CO_2 Leakage Risk Assessment of the First Chinese CCUS-EGR Pilot Project in the Maokou Carbonate Gas Reservoir in the Wolonghe Gas Field. *Energies* **2025**, *18*, 4478. https://doi.org/10.3390/en18174478

Copyright: © 2025 by the authors. Licensee MDPI, Basel, Switzerland. This article is an open access article distributed under the terms and conditions of the Creative Commons Attribution (CC BY) license (https://creativecommons.org/licenses/by/4.0/).

1. Introduction

CO_2 capture, geological storage and utilization (CCUS) is internationally recognized as one of the most effective means of mitigating global warming [1–3]. In general, CCUS is divided into three distinct components: CO_2 capture, utilization, and storage. CO_2 utilization is manifested mainly in CO_2-enhanced oil recovery (EOR) and CO_2-enhanced

gas recovery (EGR) projects, photocatalytic conversion of CO_2 [4], and biological CO_2 conversion. CO_2 storage mainly includes geologic CO_2 storage (GCS), mineralization, and marine storage, among which GCS is the most important storage method. During the process of geological storage, CO_2 may leak through several paths, such as abandoned wells, reactivated faults and caprocks [5]. The leakage of CO_2 will pollute the groundwater and subsurface soil and also has a chance of being released into the atmosphere [6–8]. Before implementing any CCUS project, conducting a CO_2 leakage risk assessment should be a top priority [9].

Several CO_2 leakage risk assessment methods were proposed recently. The available methods can be divided into qualitative and quantitative assessment methods. Qualitative risk assessment methods primarily include the following frameworks: The Containment Assurance Scenario and Significance Identification Framework (CASSIF), developed by Ferhat Yavuz et al. [10], which employs fault leakage analysis, wellbore integrity evaluation, and seal failure detection to identify critical events in geological containment systems. This framework optimizes utilization of the Features, Events, and Processes (FEP) database through real-time scenario matching, significantly enhancing the modeling accuracy of risk significance identification. The Structured What-If Technique (SWIFT) proves particularly effective for assessing risks in inaccessible hazardous environments where consequence pathways remain ambiguous. Through systematic generation of hypothetical failure scenarios, SWIFT enables preemptive risk evaluation of complex industrial operations [11]. The Vulnerability Evaluation Framework (VEF) serves as a conceptual tool for systemic vulnerability assessment. This framework assists regulatory bodies and engineering professionals in establishing customized risk metrics while providing methodological guidance for design validation, risk quantification, and regulatory compliance management [12]. Earlier CCUS leakage risk evaluations mostly used evaluation frameworks and qualitative methods due to a lack of specific data, which resulted in greater uncertainty and risk misclassification. They could not dynamically assess the real-time changes in leakage risk during the sequestration process, and had limitations in decision-making. Thus, this method is gradually being replaced by quantitative risk assessment methods [11].

Quantitative risk assessment methods effectively make up for the shortcomings of qualitative assessment methods, mainly for the realization of quantitative portrayal of the risk of leakage, such as calculating the leakage volume or the risk of leakage from a single leakage path over a certain period of time [13]. They can accurately provide input for relevant monitoring and protection measures [14]. The main quantitative risk assessment methods include the overall assessment of CO_2 leakage risk with the Performance and Risk (P&R) [15] and the main potential leakage path identification methods are the Certification Framework Approach (CFA) [16], CO_2-Predicting Engineered Natural Systems (CO_2-PENS) [17], and Risk Interference Subsurface CO_2 Storage (RISCS) [18]. The main methods used recently for assessing the risk of CO_2 leakage in CCUS-EGR projects are described in the following section, but these various methods all have certain limitations. The experimental approach includes core replacement experiments, fracture expansion and permeability tests, etc. This method offers a visual representation of the reservoir's response to CO_2 injection, but its limitations are also evident. It cannot reflect the complex geological conditions of the actual subsurface reservoir, nor can it portray the long-term evolution of the geological sealing process. The Probabilistic Risk Assessment Method (PRA) is a statistical-based approach that utilizes leakage probability statistics and Fault Tree Analysis (FTA) to quantitatively assess the risk of leakage. However, the method is inherently dependent on data, and the lack of disclosure of leakage data from the CCUS-EGR project restricts the reliability of the results due to governmental policy. Machine learning methods, as one of the key quantitative risk assessment approaches, can use neural

networks and other artificial intelligence algorithms to analyze field monitoring data from actual projects and predict leakage risk in conjunction with existing historical processes. The primary benefit of this approach is the enhanced accuracy of the calculated leakage risk probability when combined with extensive data training calculations. However, the key disadvantage is the lack of interpretability, resulting in a black-box model that hinders the provision of reliable explanations for physical mechanisms [19]. Due to the lack of sufficient evaluation data and the dynamic nature of leakage risk over time, the accuracy and timeliness of existing quantitative evaluation methods are limited.

Numerical simulation is a mature and widely used tool for data generation [20]. It uses professional numerical simulation software, such as TOUGH (Lawrence Berkeley National Laboratory, Berkeley, CA, USA), CMG (Computer Modeling Group Ltd., Calgary, AB, Canada), ECLIPSE (Schlumberger Ltd., Houston, TX, USA), etc., to construct the corresponding numerical model and accurately predict the CO_2 migration distribution and leakage risk during the process of storage [21]. The integration of risk assessment and numerical simulation holds significant potential in addressing the insufficient dynamic assessment capabilities inherent in existing quantitative evaluation methodologies.

In recent years, quantitative evaluation methods have gradually become the mainstream method of risk assessment. Aiming at the problem of wellbore leakage in the process of CO_2 geological storage in a saline aquifer, Gao et al. [22] established a quantitative risk evaluation index system based on an analytic hierarchy process so as to determine the influence weight of each influencing factor on leakage according to the score. Sorgi et al. [23] proposed a quantitative assessment method for leakage risk, which introduced measurement, monitoring and verification methods to avoid qualitative analysis or subjective judgment involved in risk assessment and analysis. Unfortunately, the method lacks actual site applicability verification. Using a quantitative analysis method, Dou et al. [24] established a heat and mass transfer and distribution model of offshore gas production wells, explored the physical process of gas leakage and migration, quantitatively evaluated the influence of different factors, and designed a series of risk prevention measures. By comprehensively comparing qualitative, semi-quantitative and quantitative methods, the qualitative evaluation method has the advantages of simple operation and short completion time, but it has poor ability in later leakage quantification and risk assessment. The semi-quantitative method can achieve advantages in operability and flexibility; the advantage of the quantitative method is that it has sufficient data persuasiveness in terms of data accuracy and uncertainty processing. The disadvantage is that the operation is difficult and the completion time is long [25]. The quantitative evaluation method established in this paper effectively solves the problem of difficult operation. Users can assign values in turn according to the scoring table and combine the existing numerical simulation results of site injection, which greatly reduces the working time.

Internationally, Enhanced Gas Recovery (EGR) technology remains at a low technological maturity level, with limited documented implementation cases [26]. Notably, China achieved a milestone in 2024 by launching its first CCUS-EGR pilot demonstration project at the Wolonghe Gas Field. Characterized by advanced technical maturity and comprehensive supporting infrastructure, this pioneering project has successfully completed the first period of CO_2 injection.

Considering the limitations and shortcomings of the above risk assessment methods, this paper focused on identifying the leakage pathways, determining the values of various leakage indicators on the overall storage risk, and combining the results of numerical simulation to propose a leakage risk assessment method for long-term CCUS projects. The Maokou gas reservoir in the Wolonghe field, southwest China, was selected as an application case to investigate the dynamic assessment results of CO_2 storage risk under

different time scales, which will provide a scientific method for field injection storage in the subsequent study area and a reliable basis for developing a leakage risk monitoring program.

2. Materials and Methods

2.1. Establishment of the Leakage Risk Assessment Method

2.1.1. Leakage Pathway Analysis

After CO_2 enters the formation through the wellbore, various factors during the injection or production may cause damage to the wellbore structure or lead to leakage along the fracture of an abandoned well. Then, the gas enters the reservoir and migrates upward due to buoyancy and accumulates under the caprock. Since the injection of CO_2 inevitably raises the pressure in both the reservoir and caprock, there is a possibility of fault or fracture activation, which in turn increases the risk of leakage [21]. With the increase of storage time, the dissolution of CO_2 in formation water and its water–rock reaction also poses a risk of changing the permeability of the reservoir's caprock [27]. Unexpected geological activities in the geological body will also damage the stability of the storage body and increase the risk of leakage. Therefore, in the above process, there will be a variety of potential leakage pathways of CO_2, mainly including the wellbore, caprock, reservoir, fault, fracture and so on (Figure 1a). Moreover, the risk of leakage through these pathways varies dynamically over time (Figure 1b). The temporal characteristics of these leakage pathways exhibit significant variability in their operational impacts. For instance, leakage through abandoned wellbores, pre-existing faults, or fractures—if it occurs—would likely manifest during the early storage phases and thus be readily detectable. In contrast, other latent risks, such as caprock integrity degradation induced by CO_2 injection-associated geomechanically stress redistribution and geochemical alteration processes, demonstrate progressive escalation with continuous CO_2 emplacement. These risks exhibit strong positive correlations with CO_2 concentration gradients. Consequently, the most effective dynamic risk quantification methodology involves integrating site-specific numerical simulations to systematically evaluate risk evolution through spatiotemporal analysis of CO_2 plume migration patterns.

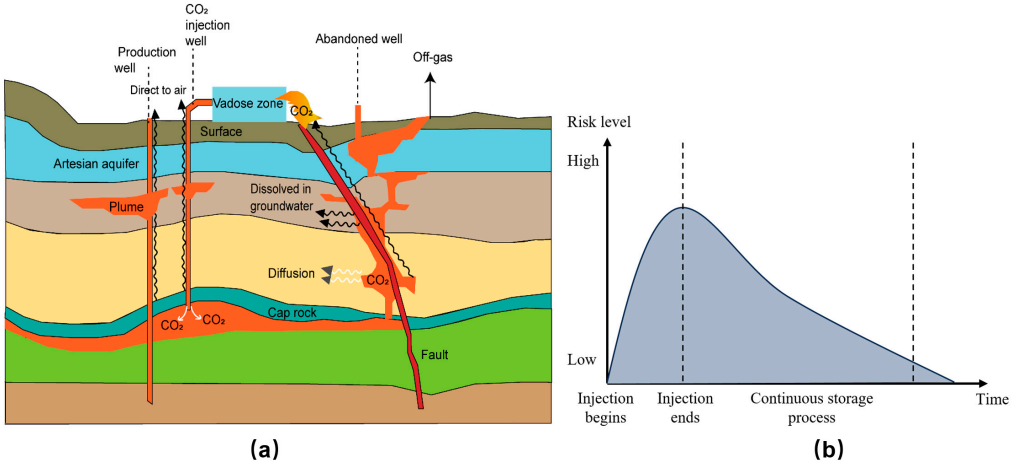


Figure 1. (**a**) Conceptual diagram of potential leakage path of CCUS, modified from Zhang et al. [28]. (**b**) Conceptual diagram of the risk of CO_2 sequestration and leakage in geological media, modified according to Gholami R et al. [29].

2.1.2. Evaluation Factors Determination

Based on the leakage pathways analysis listed above, the evaluation factors were divided into four categories: caprock, reservoir, wellbore, and geologic body safety and stability. The various evaluation factors can be further subdivided into more specific sub-factors, whose determination methods and scoring rules are shown below:

Caprock: The complete and continuous distribution of the caprock will affect the gas sequestration effectiveness in different areas of the site [30]. The thickness of the caprock can be divided into individual and cumulative caprock thickness. A greater thickness of the caprock generally correlates with enhanced safety. The permeability of the caprock directly influences the extent to which gas can escape after breaching the caprock. The lithology, mechanical stability, and chemical reactivity of the caprock mainly reflect its ability to resist external environmental changes and internal water–rock reactions over the long-term storage scale [31]. For long-term storage, it is also important to consider the content of non-reactive minerals in the caprock [32]. A series of sub-factors, including continuity, thickness, permeability, lithology, mechanical stability, and chemical reactivity, were established for accurate risk evaluation.

Reservoir: The influence of the reservoir on the overall closure performance is mainly reflected in the indirect effect on the upper caprock. The physical indices of the reservoir top adjacent to the caprock were selected to reflect this risk, in which the CO_2 mole fraction and the top pressure conditions can be used to visualize the strength of the effect on the caprock. Numerical simulations can be used to obtain the CO_2 mole fraction and top pressure distribution of the corresponding reservoir. For accurate risk evaluation, a series of sub-factors, including CO_2 mole fraction and the ratio of the top reservoir pressure to caprock rupture pressure, were established.

Wellbore: The main factors affecting the stability of a wellbore are completion time, abandonment time, cementing measures and historical accidents. The completion time determines the drilling technology and sealing methods used to complete the well [33]. The longer the abandoned time, the simpler the sealing measures taken at the time of abandonment. The quality of the cementing reflects the well's ability to withstand external interference over a long period [34]. The longer the cementing ring of the abandoned well, the better the safety of the well [5]. The last thing to emphasize is the history of technical accidents in the well. For accurate risk evaluation, a series of sub-factors were established, including the time of well completion, time of well abandonment, cementing related measures and historical engineering accidents.

Geological body safety: The main factors affecting the safety of the storage system include existing faults, potential rifts and seismic risk. As the dominant leakage path, a fault will greatly increase the risk of sealing leakage [35,36]. The peak acceleration of ground vibration is the horizontal acceleration corresponding to the maximum value of the ground vibration acceleration response spectrum. A smaller value indicates better overall safety and stability of the storage [37]. For accurate risk evaluation, a series of sub-factors including existing faults, potential rifts and peak acceleration were established.

2.1.3. Scoring Rules of the Sub-Factors

The scoring rules of sub-factors follow the principle of uniformity and grading according to the degree of influence on the leakage of the safety risk of the storage body. The greater the influence, the lower the score, with a minimum of 0.2, and the smaller the influence, the higher the score, with a maximum of 1. After that, the score will be graded according to the degree of influence, including 0.8, 0.6, 0.4 and so on. The specific scores of the risk levels are shown in Table 1.

The continuity of the caprock can be roughly categorized into three levels [30]. The thickness of the single layer at the bottom of the caprock is classified into three levels. The cumulative thickness of the caprock is divided into three classes. The caprock permeability is divided into three grades. The lithology of the caprock is divided into four grades according to the mud content. The mechanical stability of the caprock is divided into

four grades. The chemical reactivity of the caprock is reflected by the content of non-reactive mineral content, which is roughly divided into four grades [32].

Table 1. Scores in relation to risk level.

Score	Risk Level
0.2	high
0.4	relatively high
0.6	medium
0.8	low
1.0	free

The CO_2 mole fraction is divided into five grades. When the top reservoir pressure approaches the caprock rupture pressure, the risk of rupture increases, which is divided into four grades.

The well completion time can be categorized into three grades. Wellbore abandonment time is divided into three grades on the basis of different times. The quality of cementing is qualitatively divided into three grades [34]. Finally, the history of accidents in wellbore is divided into three categories.

The distribution of faults or fractures in the caprock and reservoir can be classified into four grades on the basis of their scale. The grading of peak ground shaking acceleration is divided into five grades according to the actual seismic regions in China.

2.1.4. Evaluation Parameter Obtaining and Scores Calculation

The parameters of the caprock category index must be obtained from the corresponding stratigraphic data of the study area. The parameters in the wellbore category index and geological body safety category index, such as completion time and peak ground shaking acceleration, must be combined with the actual engineering situation, which can be obtained by consulting relevant data. The CO_2 mole fraction and pressure at the top of the reservoir, as part of the reservoir category index, need to be obtained with numerical simulation. The formation rupture pressure can be calculated using the Eaton method [38] based on the reservoir formation pressure evaluation method (Equation (1)):

$$P_f = \frac{\mu}{1-\mu}(P_0 - P_P) + P_P \quad (1)$$

In the formula:

P_f is the formation rupture pressure, MPa;

μ is the Poisson's ratio of the stratum, dimensionless;

P_0 is the overlying stratum pressure, MPa;

P_p is the formation pore pressure, g/cm^3.

The caprock juxtaposition thickness by fault is used to quantitatively characterize the vertical development of faults (Equation (2)) [36]:

$$H_j = H_c - H_f \quad (2)$$

In the formula:

H_j is the caprock juxtaposition thickness, m;

H_c is the caprock thickness, m;

H_f is the fault vertical throw, m.

During the process of geological storage, once a certain pathway leaks, it will cause huge safety hazards to the overall storage unit and even cause a series of malignant

continuous safety accidents due to gas leakage. Therefore, we must consider the risks of each index equally.

The cumulative multiplication method is then adopted to comprehensively evaluate the CO_2 leakage risks by multiplying all indicators' scores, emphasizing time-amplified leakage impacts on system integrity as illustrated in Equation (3). Lv et al. [6] believed that there were differences in the hazard levels caused by different leakage pathways, and the scoring method was optimized on the basis of referring to the results of hazard classification. The corresponding evaluation score index coefficients were formulated for different types of leakage routes: wellbore, fault and geological activity are the first-level hazard indicators, and all sub-indicators need to be squared after multiplying the scores; the caprock and reservoir are the secondary hazard indicators, and the corresponding sub-index index coefficient is 1, that is, it remains unchanged.

$$\mathrm{SF} = (S_W * S_G)^2 * S_C * S_R \quad (3)$$

In the formula:

SF is the safe factor, which is equal to the result of multiplying the scores of all indicators in the assignment table;

S_w is the cumulative multiplication of score values of all wellbore indexes, given by the assignment table;

S_G is the cumulative multiplication of score values of all geological body safety indexes, which combines caprock faults, reservoir faults, and peak ground acceleration;

S_C is the cumulative multiplication of score values of all caprock indexes, given by the assignment table;

S_R is the cumulative multiplication of score values of all reservoir indexes, given by the assignment table.

The calculated SF classifies the risk into low, medium or high leakage levels, as outlined in Table 2.

Table 2. CO_2 leakage risk classification.

CO_2 Leakage Safety Index Calculation Results	Risk Level
0.1–1	low
10^{-4}–0.1	medium
$<10^{-4}$	high

2.2. CO_2 Leakage Risk Assessment of the Wolonghe CCUS-EGR Project

2.2.1. Background

The Wolong gas field is located in the Chongqing Changshou District, where the exposed Jurassic sand mudstone strata of the Ziliujing Group Dongyuemiao section represent the most ancient stratification. The gas field was first put into trial production in January 1972, and as of February 2023, the Wolonghe gas field had a cumulative total of 129 completed wells, with a cumulative gas production of 359.07×10^8 m^3. Utilizing this gas field as a paradigm, it is proposed that CO_2 geological storage be employed in conjunction with enhanced oil and gas recovery (CCUS-EGR).

This project is the first natural gas purification plant and gas carbon capture industrialization project in China, and it is also the first demonstration project of injecting CO_2 for enhancing natural gas recovery. Its carbon capture device is the first low pressure, medium and low concentration carbon capture device in China. The project adopted the mode of CCUS-EGR, and the chemical absorption method was used to capture the CO_2 discharged

from the exhaust gas treatment unit. It is anticipated that about 26,500 tons of CO_2 can be captured annually and the gas recovery can be enhanced by 10% via CO_2 injection.

2.2.2. Numerical Model Establishment and Parameter Obtaining

The numerical model of the W67 well zone located in the Maokou Formation of the Wolonghe gas reservoir was established as shown in Figure 2. The professional reservoir simulation software CMG was employed by adopting the deterministic modeling method and the actual parameters were used to construct the geological model, which includes the well coordinates and the level structure, fault, well slope, geological layering, porosity, permeability and gas saturation data. At the same time, the quality of the geological structure, fault distribution and drilling stratification were strictly controlled, and the planar grid was dissected with a size of 50 m × 50 m. The basic parameters of the model are shown in Table 3.

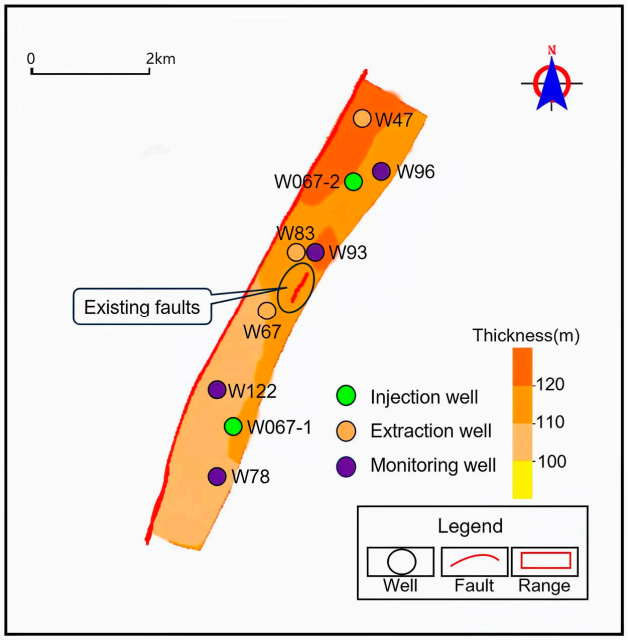


Figure 2. Thickness of caprock, well placement, and distribution of existing faults in the study area.

Table 3. Reservoir component model parameters and values.

Parameter	Value	Parameter	Value
surface area	19.7 km^2	permeability	0.1–134 mD
stratum	Maokou Group II	storage temperature	85.74 °C
central burial depth	3477 m	wellbore distribution	3 wells center,4 wells side
storage pressure	54.639 MPa	injection gas	Pure CO_2
gas reserves	66.2 × 10^8 m^3	number of wellbores	7
porosity	0~10%	number of grids	460,000

The caprock of the gas reservoir is the Longtan Formation, which consists of dense mudstone. The distribution is continuous, with a thickness of about 100~130 m. Its average permeability and porosity are 9.5 × 10^{-9} mD and 0.00385, respectively. The caprock does not contain reactive minerals and its mechanical properties are stable and not deformed.

The main component of reservoir gas is methane, accounting for 96.57%, while the remaining impurity gases are CO_2 and H_2S, accounting for 2.11% and 0.77%, respectively. The gas field is a dry gas reservoir characterized by ultra-low water saturation, with original connate water saturation ranging from 6.6% to 12.6%.

The permeability distribution of the numerical model relies on logging permeability data, and it was analyzed and calculated for different areas using well test data. The porosity distribution was derived from the logging porosity data and was analyzed using the sequential Gaussian simulation algorithm. The specific spatial distributions of the permeability and porosity are shown in Figure 3.

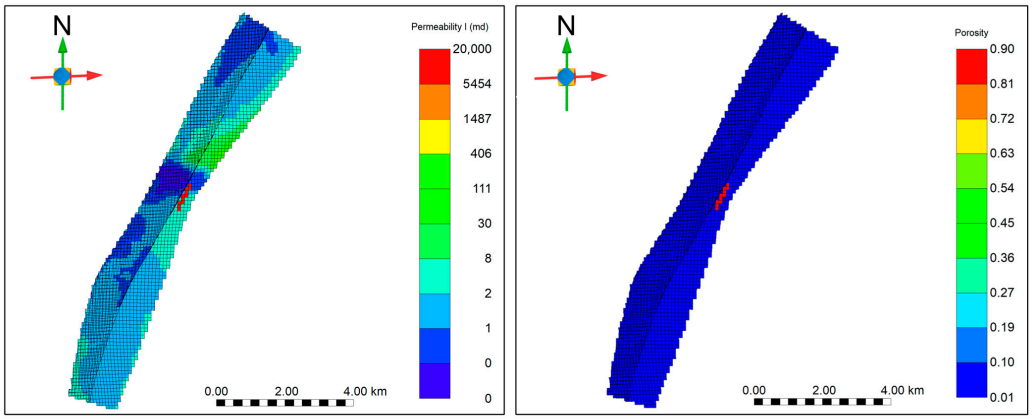


Figure 3. Permeability (**a**) and porosity (**b**) distribution of the Wolonghe gas field W67 well zone.

There are two injection wells (W067-1 and W067-2) and three production wells (W47, W83, W67) located in the study area, as shown in Figure 2. The results of the cementing quality survey showed that there are 14 existing old wells, 10 wells that qualified for the pressure test, 2 wells that have no cementing quality test data and 2 wells that are unqualified (as shown in Table 4). All of the wells are now in a normal working condition, except for W122, which was abandoned in 2007.

Table 4. Wellbore information.

Well Number	Well Type	Establishment Time
W47	extraction well	1977
W83	extraction well	1985
W67	extraction well	1978
W93	monitoring well	1985
W122	monitoring well	2004
W78	monitoring well	1985
W067-1	injection well	2022
W067-2	injection well	2022

There is only one NE-SW fault in the gas production area of the W67 well, with a planar extension length of about 800 m. According to the relevant information, the seismic defense intensity of this site is 6 degrees, and the value of ground shaking acceleration is 0.05 g.

This CO_2-EGR project was planned into two phases. For phase I (2022–2027), a per-well CO_2 injection rate of 100,000 m^3/day and an aggregate production rate of 70,000 m^3/day for production wells were selected. During Phase II (2027–2053), representing the expansion phase, the injection rate was 150,000 m^3/day per injection well, while the total production rate was elevated to 110,000 m^3/day.

2.2.3. Leakage Scenarios Set up

Based on the identification and analysis of leakage paths, this paper established a leakage risk assessment framework. However, in the actual storage process, various

unpredictable sudden leakage situations may occur. Therefore, it is necessary to select representative indicators in the evaluation framework and combine them with the actual engineering situation to predict possible leakage scenarios. This measure can provide a reliable basis for verifying the accuracy and applicability of the evaluation framework to a certain extent.

Building upon the risk assessment indicators and the actual conditions of the study area (as shown in Figure 2), three scenarios, namely, CO_2 leakage along the well, leakage when the cap layer is damaged by faults, and new faults generation in the reservoir were set up. The detailed parameter settings in different scenarios are listed in Table 5.

Table 5. Parameter settings for different simulation groups.

Division of Groups	Longitudinal Extension of the Fault to the Length of the Cap
Control group	No fault
Experimental group a	50 m
Experimental group b	100 m
Experimental group c	200 m

Leakage along the wellbore: In order to simulate leakage along the injection well, a specific grid near the injection well was set as a single fracture. The permeability of the fracture grid is 20,000 mD, the porosity is 0.9, and the rest of the parameters are consistent with the original model [39].

Leakage from new faults in the reservoir: The new fracture network at the edge of the gas production area was used to simulate the addition of new faults caused by geological activity. The permeability of the fracture network is 20,000 mD, the porosity is 0.9, and all other parameters are the same as in the original model.

Leakage of caprock damaged by faults: Three simulation groups (a, b, and c) were set up, with fault longitudinal extension thicknesses of 50 m, 100 m, and 200 m, respectively (Table 5 and Figure 4). These groups simulated different fault extension distances triggered by varying levels of geological activity. The permeability of the fracture grid is 20,000 mD, the porosity is 0.9, and all other parameters remain consistent with the original model.

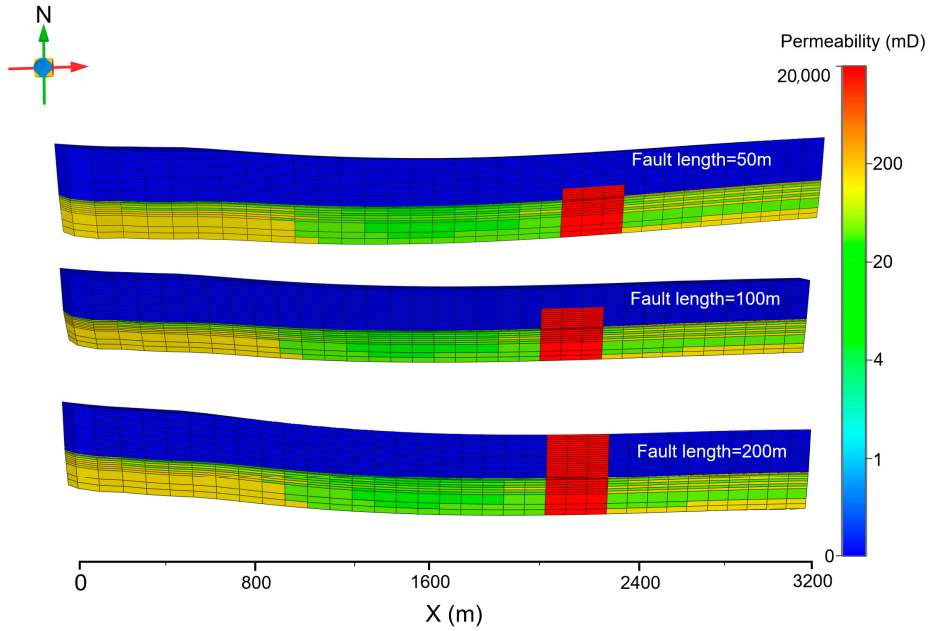


Figure 4. Longitudinal cross section of the caprock in different experimental groups (caprock layer in blue, reservoir in yellow–green, fault in red).

3. Results and Discussion

3.1. CO_2 Dynamic Leakage Risk Assessment Framework

Aiming at the identified factors and sub-factors, the grading assignment method was used to determine the corresponding scores of different levels according to the influence of different indicators on the leakage risk. The specific scoring rules for different risk factors are shown in Table 6.

Table 6. Sequestration system risk scoring of indicators.

Class I Indicators	Class II Indicators	Basis of Classification	Corresponding Score
Caprock	Caprock integrity continuity	Cover trap area > 80% and no broken area	1
		Cover trap area 40–80%	0.8
		Cover trap area < 40%	0.4
	Thickness of a single cap layer immediately adjacent to the reservoir	>20 m	1
		10–20 m	0.8
		<10 m	0.6
	Cumulative caprock thickness	>300 m	1
		150–300 m	0.8
		<150 m	0.6
	Caprock permeability	$<10^{-3}$ mD	1
		10^{-3}–10^{-2} mD	0.6
		$>10^{-2}$ mD	0.4
	Caprock rock type	Paste rock, mudstone, calcareous mudstone	1
		Sandy or silty mudstone	0.8
		Sandy mudstone, silty mudstone	0.6
		Shale, dense graywacke	0.4
	Caprock mechanical stability	Rock Young's modulus > 18 Gpa	1
		Rock Young's modulus 15–18 Gpa	0.8
		Rock Young's modulus 12–15 Gpa	0.6
		Rock Young's modulus < 12 Gpa	0.4
	Caprock non-reactive mineral content	>80%	1
		60–80%	0.8
		40–60%	0.6
		20–40%	0.4
		0–20%	0.2
Reservoir	The CO_2 mole fraction of top reservoir	0–10%	1–0.9
		10–30%	0.9–0.7
		30–50%	0.7–0.5
		50–70%	0.5–0.3
		70–100%	0.3–0
	Top reservoir pressure/caprock rupture pressure	0.4–0.5	1
		0.5–0.6	0.8
		0.6–0.8	0.6
		>0.8	0.4

Table 6. *Cont.*

Class I Indicators	Class II Indicators	Basis of Classification	Corresponding Score
Wellbore	Wellbore engineering project	Non-existent	1
		Existent	0.4
	Wellbore completion time	Completion time < 18 years	1
		Completion time > 18 years but completed after 1992	0.8
		Completed before 1992	0.4
	Wellbore abandonment time	Less than 5 years	1
		5–13 years	0.8
		More than 13 years	0.6
	Wellbore cementing quality	Excellent cementing quality	1
		Medium cementing quality, partially disconnected free well sections	0.8
		Poor cementing quality, generous connected free well sections	0.4
	Cementing depth of cemented ring	Sealed to surface	1
		Unsealed to surface	0.6
	Length of cement ring cementation for abandoned wellbore	>30 m	1
		5–30 m	0.8
		0–5 m	0.6
		No measures taken	0.2
	Wellbore historical engineering incidents	All free of engineering incidents	1
		Technical events such as overflows and well surges	0.6
		Had well blowout	0.2
Geological body safety	Fault or rift development in the caprock	No faults or fractures	1
		H_j > 100 m	0.8
		H_j 50–100 m	0.6
		H_j < 50 m	0.4
	Fault or rift development in the reservoir	No faults or fractures	1
		Limited faults and intact caprock	0.8
		5–10 large-scale faults (extending more than 1 km)	0.6
		More than 10 large-scale faults or have fracture zone (extending more than 1 km)	0.4
	Peak ground acceleration	<0.05 g	1
		0.05–0.1 g	0.8
		0.1–0.2 g	0.6
		0.2–0.3 g	0.4
		>0.3 g	0.2

3.2. Validation of the Numerical Model of the Wolonghe EGR Project

It is important to validate the established numerical model with historical production data to guarantee the accuracy and scientific validity of the simulation results. In this paper,

the historical gas production rate of W47 and wellhead pressure were employed to calibrate the numerical model by model fitting, and the fitted results are shown in Figure 5.

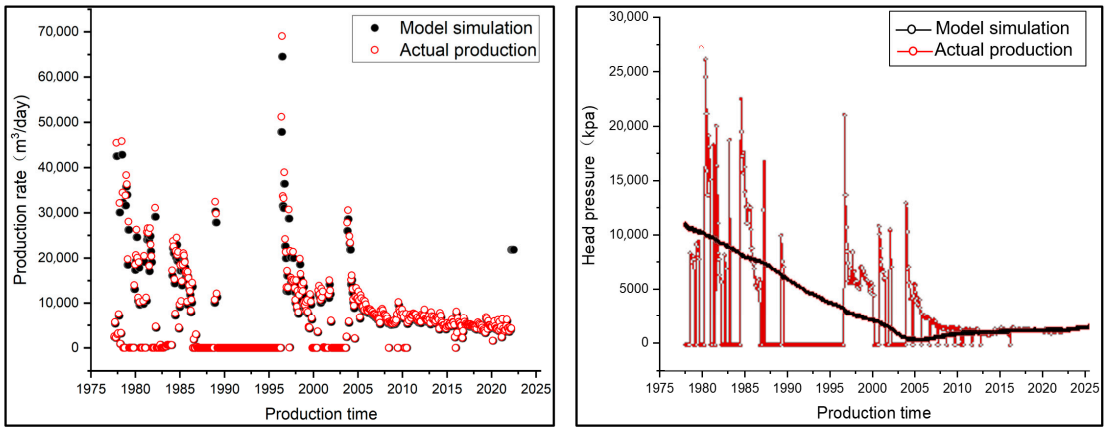


Figure 5. Model production rate and pressure fit for well W47. ((**a**) is W47 production rate validation results; (**b**) is W47 head pressure validation results).

The fitting results on gas production rate show good agreement with the historical data, especially after 2005. In the early stages of production, due to the lack of historical data, there is a large error between the simulated and actual values of wellhead pressure. However, with the enrichment of production data samples after 2010, the fitting results of wellhead pressure have become increasingly realistic. Overall, it can be seen that the numerical model constructed in this paper demonstrates a good historical fitting effect. The model is accurate and reliable, and the simulation results obtained can be used as an important basis for subsequent risk assessment and the development of monitoring programs.

3.3. Simulation Results Under Normal Operating Conditions

The simulation results of the CO_2 mole fraction distribution at the top of the reservoir for 5 years of gas injection, 10 years of gas injection, and 30 years of gas injection under normal operating conditions are shown in Figure 6.

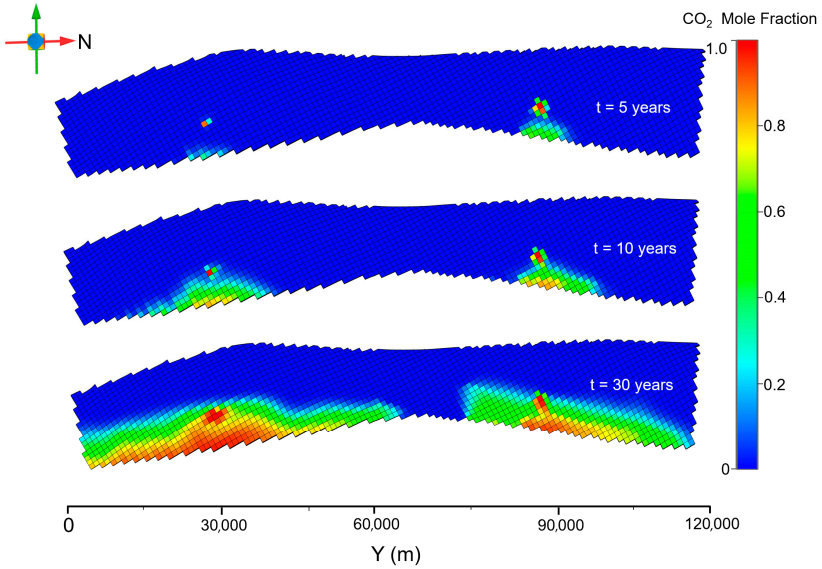


Figure 6. CO_2 distribution at the top of the reservoir at different gas injection times under normal operating conditions.

The permeability distribution of the reservoir exhibits a distinct pattern of higher values in the eastern region compared to the western region, consequently leading to preferential eastward migration of injected CO_2 (Figure 6). Figure 7 shows the CO_2 migration distance at different times of gas injection. For phase I (injection rate: 100,000 m^3/day, duration: 5 years), the analysis reveals that the maximum north–south migration distance of CO_2 from the southern injection well reaches approximately 10,000 m, while the northern injection well demonstrates a greater migration extent of 12,000 m along the same orientation. Additionally, a discernible migration plume extending approximately 8000 m from the injection wells toward the eastern boundary is observed. After 10 years of continuous injection, the migration distances exhibit a progressive enlargement. The southern injection well shows a significant increase in north–south migration distance, reaching 16,000 m, whereas the northern counterpart reaches 14,000 m. The CO_2 plume maintains its eastward migration tendency toward the boundary. Reaching 30 years of injection duration, both injection wells demonstrate extensive CO_2 migration. The maximum north–south migration distances escalate to 30,000 m (southern well) and 25,000 m (northern well), respectively. Notably, the eastward migration distance from injection wells to the eastern boundary attains 10,000 m. The overall spatial distribution consistently manifests higher migration potential in the eastern sector relative to the western region, aligning with the inherent permeability characteristics of the reservoir.

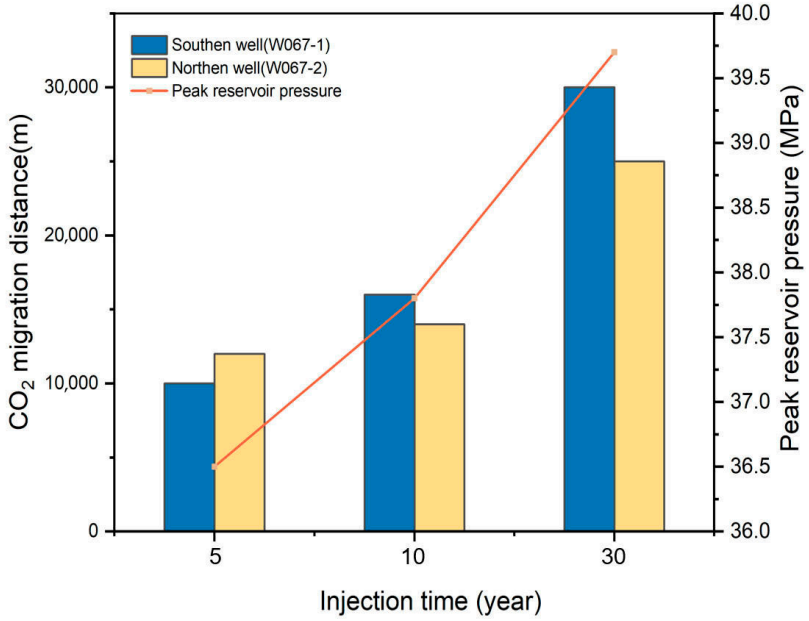


Figure 7. CO_2 migration distance and peak pressure of the reservoir at different times of gas injection.

Pressure variations induced by CO_2 injection constitute a critical monitoring parameter. Figure 7 shows the peak pressure curve and Figure 8 illustrates the spatiotemporal evolution of reservoir pressure under normal operating conditions across different injection durations. The spatial pressure distribution demonstrates a strong positive correlation with the CO_2 plume dispersion pattern. At the 5-year injection period, the maximum reservoir pressure reaches 36.5 MPa, escalating to 37.8 MPa after 10 years of continuous injection. Upon reaching 30 years of sustained injection, the formation pressure peaks at 39.7 MPa. Notably, short-term injection (<5 years) induces minimal pressure deviation from initial formation conditions, whereas the 30-year injection duration triggers a marked pressure surge in the eastern sector. This results in a distinct west-to-east pressure gradient, consistent with the reservoir's intrinsic permeability anisotropy.

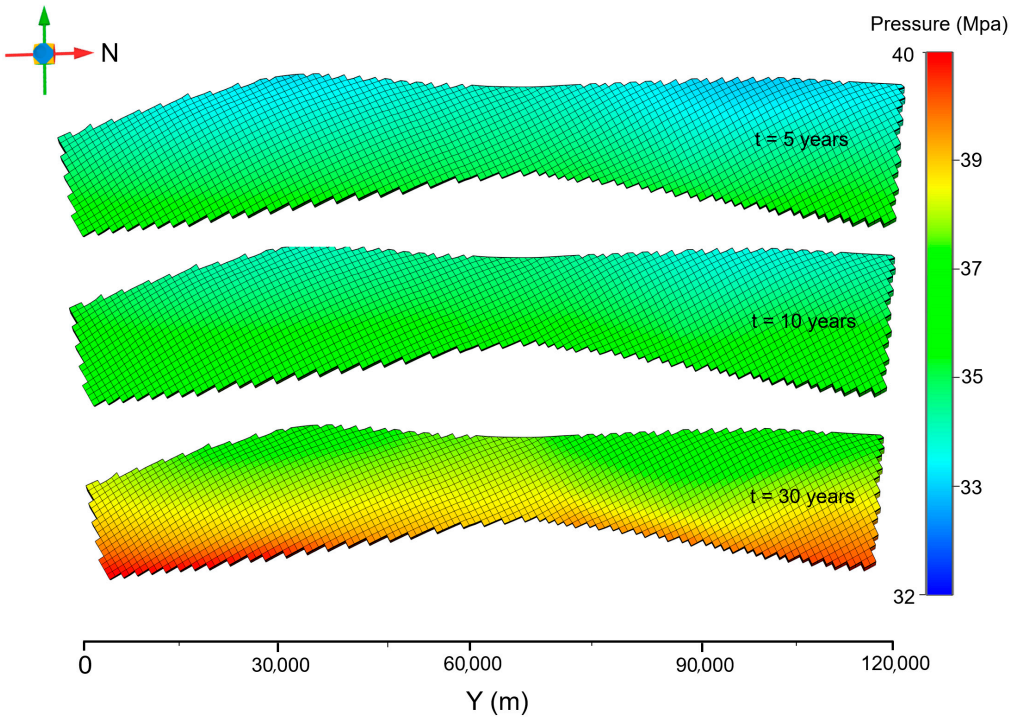


Figure 8. Pressure distribution at the top of the reservoir at different times of gas injection.

The reservoir exhibits ultra-low water saturation characteristics (ranging from 6.6% to 12.6%), significantly suppressing geochemical reaction intensities under current conditions. Because of the unique carbonate reservoir in the study area, numerical simulation was used to investigate the effect of the CO_2 water–rock reaction process on the amount of CO_2 leakage via the cap rock, as shown in Table 7.

Table 7. Comparative analysis of CO_2 leakage capacity under different scenarios (t).

	Water–Rock Reaction	No Water–Rock Reaction	Relative Change	Average Annual Change
10 years	1.01	1.14	0.13	0.013
20 years	9.68	10.56	0.88	0.044
30 years	32.65	35.33	2.68	0.089

From Table 7, it can be seen that the partial CO_2 leakage from the caprock after the addition of the water–rock reaction is slightly less than that from the cap without the addition of the water–rock reaction. Considering that some of the CO_2 may dissolve simultaneously, it is assumed that part of the CO_2 also passively participates in the mass consumption of the water–rock reaction process, which reduces the mass of gas diffused into the caprock, and the amount of CO_2 leakage from the caprock may be reduced. The average annual change in the leakage mass of the two is less than 0.1 t over a longer reaction time, which is a very small error compared to the uncertainty of the real situation over a long-time scale simulation. Therefore, it can be assumed that the CO_2–water–rock chemical reaction has a relatively small impact on the caprock. For this reason, water–rock interactions were excluded from the analytical framework due to their negligible thermodynamic impact.

3.4. CO_2 Leakage Under Different Leakage Scenarios

3.4.1. Spatial Distribution of CO_2 Under Different Scenarios

The CO_2 distribution at the top of the reservoir under the wellbore leakage scenario is shown in Figure 9. The maximum north–south migration distances show minimal variation

from those under normal operating conditions; however, significant divergence is observed in both the maximum CO_2 mole fraction value and the spatial distribution patterns of high-concentration CO_2 accumulation zones during equivalent operational timeframes. According to the simulation results, 5 years after CO_2 injection begins, the CO_2 gas fraction in the fracture network of the reservoir appears to be significantly increased due to the presence of fractures in the injection well. The maximum mole fraction is only about 0.8. In contrast, there is no large-scale high-concentration CO_2 accumulation zones at the top of the reservoir. After 10 years of injection, the CO_2 shows a tendency to diffuse from the fracture to the surrounding area and the maximum fraction increases to 1.0. When the gas injection time reaches 30 years, the gas concentration in most of the grid appears to increase sharply, and the high gas concentration zone is concentrated near the two injection wells, showing a migration trend from a low concentration in the west to a high concentration in the east. The CO_2 migration area expands to an impressive 1100 km^2.

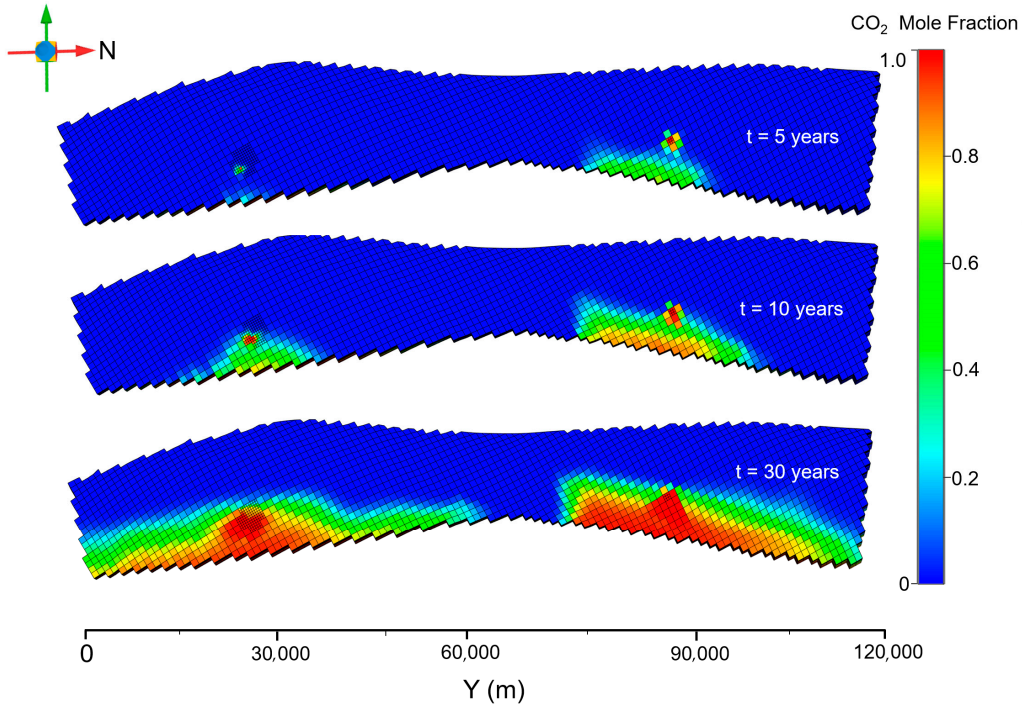


Figure 9. Wellbore leakage scenario CO_2 distribution at the top of reservoir for 5, 10 and 30 years of gas injection.

When compared to the no fracture control group, the presence of fractures in the injection well may reduce the concentration of gas components in the original migration grid. However, excessive gas concentrations concentrated near the fracture can lead to a greater susceptibility to excessive gas pressures at specific points, increasing the risk of caprock breach at particular points.

The CO_2 distribution at the top of the reservoir in the caprock leakage scenario is shown in Figure 10. The maximum north–south migration distances demonstrate minimal variation from those under normal operating conditions. By comparing the simulation results, it is found that the damage to the caprock caused by faults has less influence on the distribution of CO_2 gas in the reservoir. The spatial distribution of CO_2 is basically the same as the normal working condition.

The CO_2 distribution at the top of the reservoir in the fault leakage scenario is shown in Figure 11. After 5 years of gas injection, the total amount of injected gas is small, and the presence of new faults buffers the high-pressure area generated by the gas injection. The concentration of CO_2 components decreases significantly in the area close to the new fault,

presumably because the presence of the fault promotes gas migration to the surrounding grids and the upper caprock. After 30 years of gas injection, the CO_2 content in the grid at the top of the reservoir near the injection well area increases significantly. The decrease in gas content in the fault grid indicates that this part of the gas has already diffused into the upper caprock, which increases the possibility of gas leakage from the cap layer.

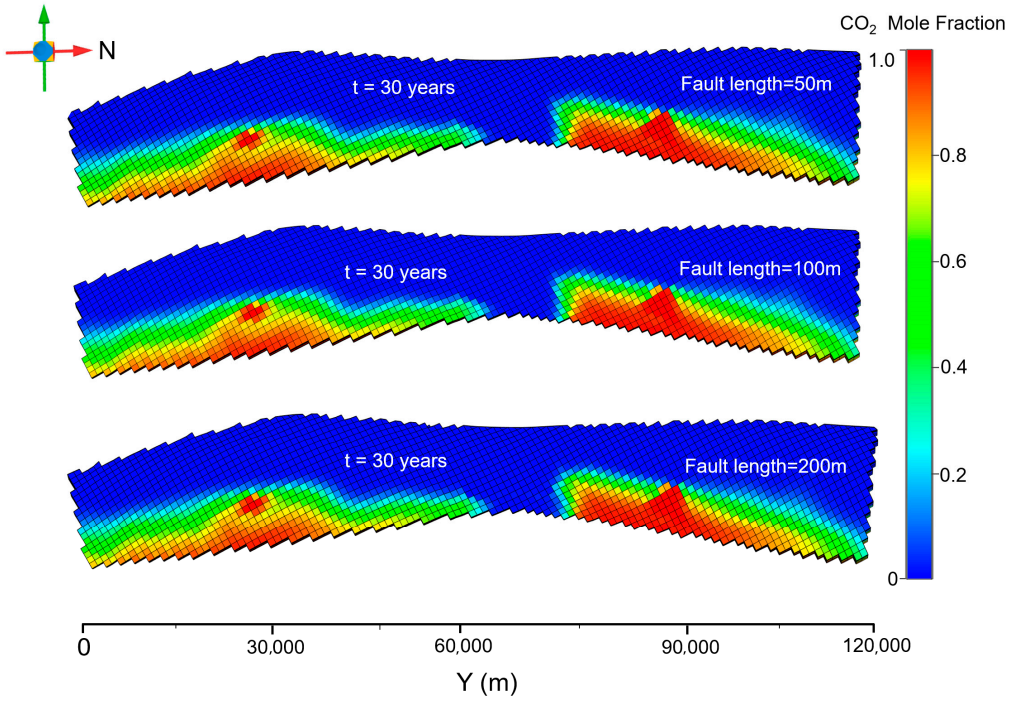


Figure 10. Caprock leakage scenario CO_2 distribution at the top of reservoir for 30 years of injection in different groups.

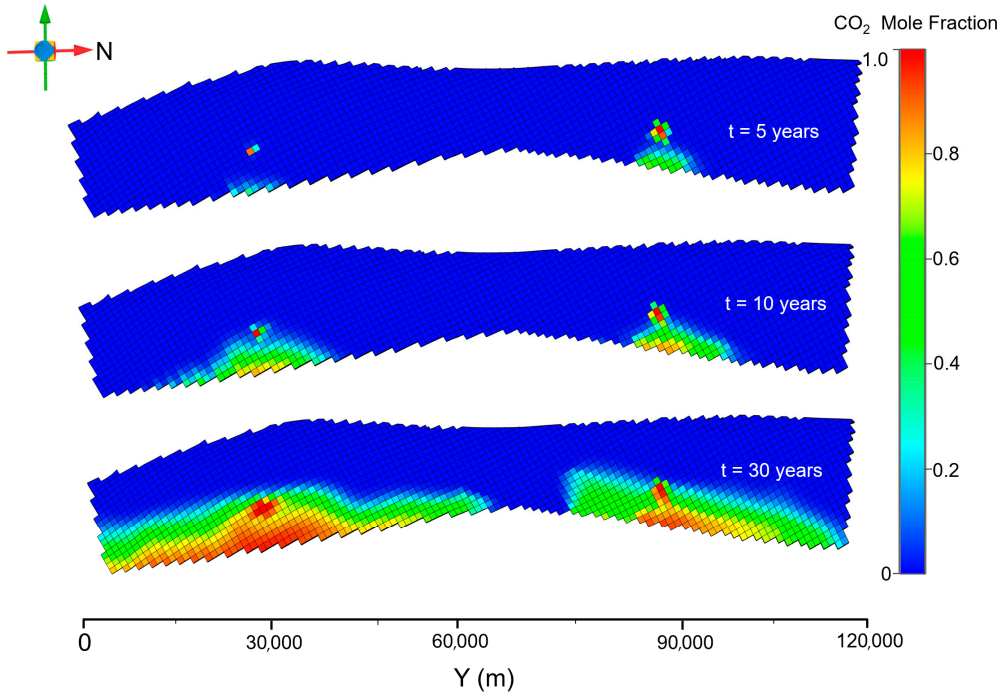


Figure 11. Fault leakage scenario CO_2 distribution at the top of reservoir for 5, 10 and 30 years of gas injection.

3.4.2. Leakage Capacity of CO_2 via the Caprock Under Different Leakage Scenarios

The results of the CO_2 leakage calculations for the caprock section are shown in the Table 8. The presence of fractures in the injection wells exacerbates the process of CO_2 leakage in the caprock formation, and the amount of leakage generated by a small volume of fractures is extremely large, far exceeding that of the control group by a factor of 600. Moreover, the presence of new faults does not have a significant effect on CO_2 leakage in the caprock. Even with an injection time of up to 30 years, the difference is very small. As long as reservoir faults do not disrupt the upper caprock, some smaller-scale additions to the reservoir area will not affect the caprock's sealing capacity.

Table 8. Caprock CO_2 leakage capacity (t) under different scenarios.

Injection Time	Control Group	Wellbore Fracture Group	Sim. a	Sim. b	Sim. c	New Fault Group
5 years	0	1635.7	110.03	178.64	296.75	0
10 years	0	4936.8	232.67	388.26	652.96	0
30 years	8.4	26,278.2	892.58	1591.83	1800.92	5.19

As shown in Figure 12, a more accurate quantitative assessment of the gas leakage is provided. During the 30 years injection period, the CO_2 leakage in the experimental group is up to 160–320 times higher than that of the control group. It can be seen that the gas leakage increases sharply as the injection time increases, and the length of the flaw extending into the caprock also affects the leakage amount. When the fault destroys the entire caprock, the integrity and sealing of the cap layer will no longer exist.

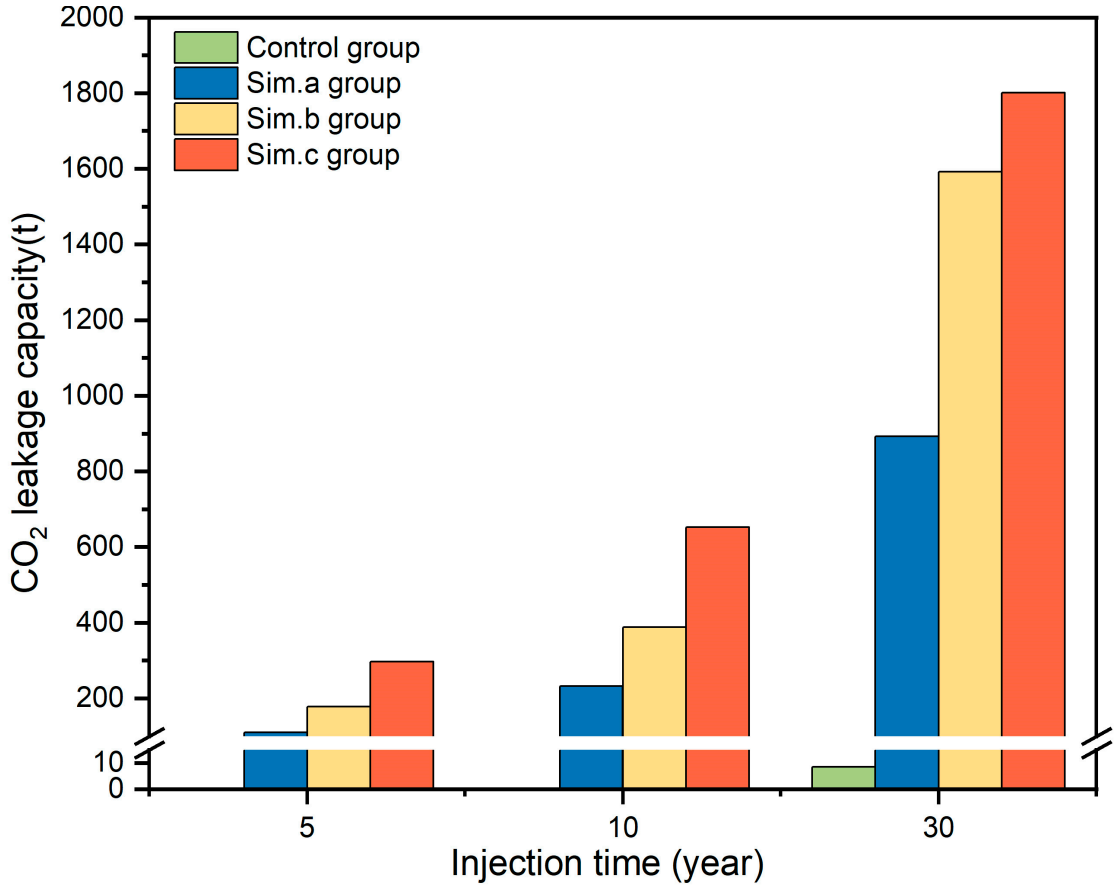


Figure 12. Comparison of CO_2 leakage from caprock under different leakage scenarios.

3.5. Sensitivity Analysis

The sensitivity analysis of the simulation in this paper is mainly divided into two categories: a sensitivity analysis of the actual site and a sensitivity analysis of the leakage path. For the verification of the actual site model, this paper fully investigated the geology data, constructed the regional scale model based on the actual stratum conditions, and completed accuracy verification of the model based on the historical production data. It can be considered that the model parameters are fully applicable to the actual site.

Secondly, this paper focused on the main leakage path in the geological storage process. After establishing the model, the representative leakage situation was selected for simulation prediction. The prediction results also further reflect that the caprock is the dominant factor determining storage risk. Other model parameters were less sensitive to the overall storage, which verifies that the evaluation scoring mechanism established in this paper is feasible.

3.6. Leakage Risk Assessment of the Wolonghe CO_2-EGR Project

On the basis of the different working stages of the injection and extraction wells in the actual sequestration process, the leakage risks at 5 years after the start of injection (2027) and 30 years after the expansion of the injection volume (2053) were calculated and the corresponding risk grading diagrams were drawn.

According to the leakage rating method in Table 6, a higher score indicates a safer containment process. Areas with a risk score greater than 0.1 have a low risk of leakage and are acceptable under normal working conditions. Conversely, areas with a risk score of less than 0.1 have a higher potential risk of leakage.

With an injection time of 5 years, the potential leakage risk is mainly located in the vicinity of the W83 and W93 wells, which were analyzed due to the poor cementing quality of the W83 wells, and there is a risk of leakage along the wellbore. Another potential risk point is near the W47 well, where poor cementing quality in the B and C annulus of the well increases the risk of gas leakage. In addition, the risk of leakage around the two injection wells is also high, and it is recommended that appropriate monitoring programs be implemented. Overall, the leakage risk is very low under the condition of 5 years of gas injection and the containment is in an ideal sealing condition. However, individual engineering wells may increase the leakage risk in the adjacent area due to the time of well formation and cementing quality. Therefore, it is necessary to strengthen monitoring efforts and take the necessary preventive measures.

In the second stage of extending injections to 2053, the points with potential leakage risk show a regionalized increase, mainly distributed on the eastern side of the study area. The analysis suggests that there are some areas of higher permeability on the east side of the reservoir, forming a dominant permeability path. The process of sequestration promotes further gas migration, which increases the risk of leakage when the caprock is breached. Overall, as storage time and the total amount of injected gas increases, CO_2 will eventually accumulate at the top of the reservoir due to its own buoyancy, significantly increasing the average molar fraction of CO_2 and the formation pressure. Referring to the scoring rules in Table 2, the overall score is significantly lower compared to 2027, which is consistent with the increased risk of leakage after actual injection. For long-term storage, the high-risk areas shown in Figure 13 need to be equipped with appropriate monitoring points to track the leakage risk in real time, ensuring that the dangerous situation at individual risk points does not deteriorate, which could lead to a dramatic spread of gas in the local area or even throughout the entire study area.

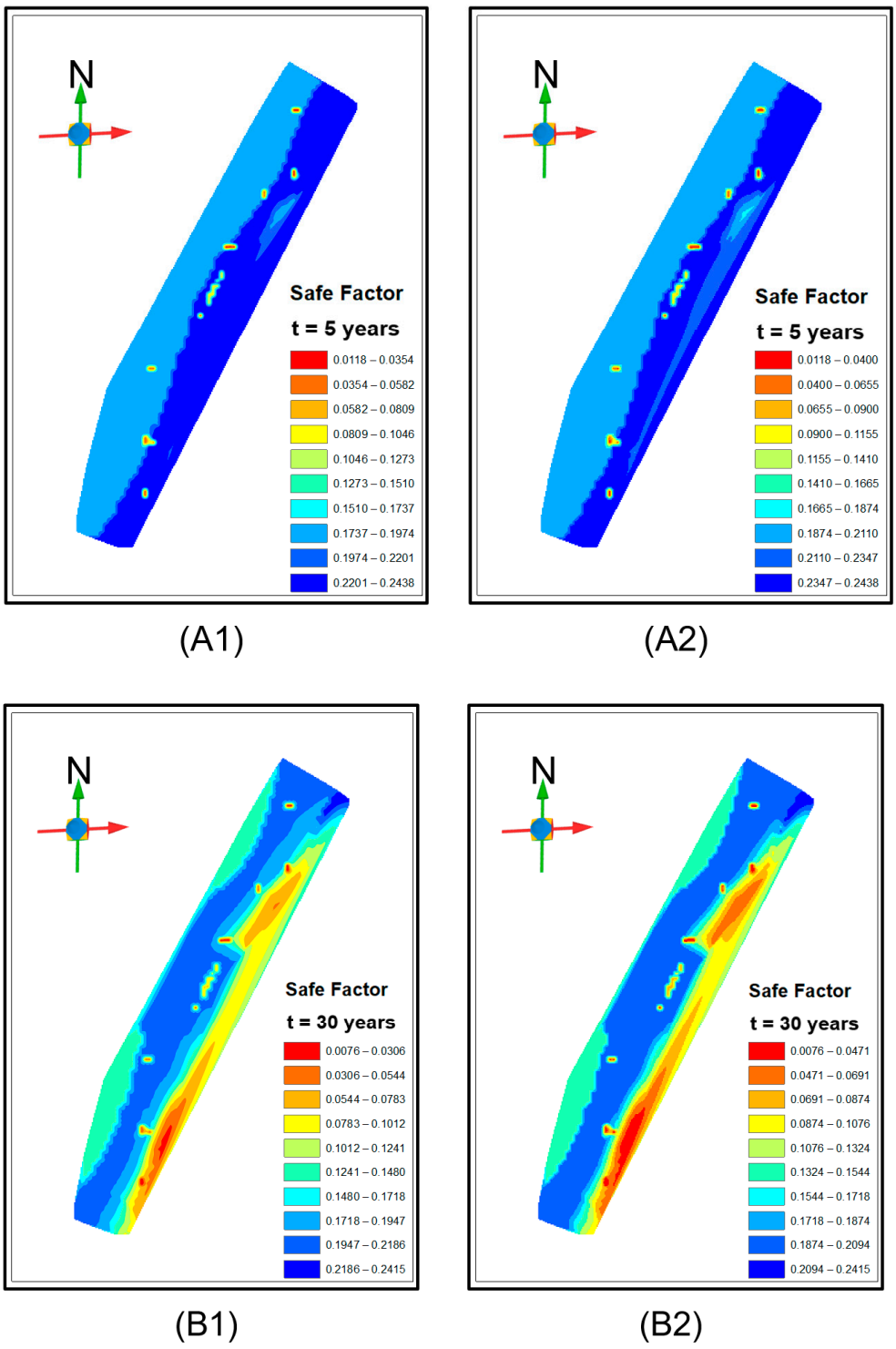


Figure 13. Map of safe factors for the study area at different injection times ((**A1**) is the safe factor spatial distribution at 5 years injection; (**B1**) is the safe factor spatial distribution at 30 years injection; (**A2**) and (**B2**) are the safe factor plots after superimposing the spatial distribution of CO_2 mole fraction).

4. Conclusions

This paper proposed a dynamic assessment method for CO_2 leakage risk assessment and applied it to the CO_2-EGR project in the Wolonghe gas field, which is the first CO_2-EGR pilot project in China. The conclusions are summarized as follows:

(1) Considering the necessity of constructing a numerical model for each CCUS project, a more precise dynamic evaluation method for assessing CO_2 leakage risk was developed. A

comprehensive evaluation index and a scientific score calculation method were established according to the characteristics of different leakage modes and their influencing factors.

(2) An accurate 3D numerical model of the CO_2-EGR project in the Maokou gas reservoir was developed and validated using detailed geological and hydrological data and historical production data. The CO_2 leakage risks under different scenarios were evaluated and the results indicated that the CO_2 leakage risk was observed to be most pronounced when the caprock integrity was damaged by faults or geologic activities. This was followed by leakage caused by wellbore failures.

(3) According to the dynamic CO_2 leakage risk assessment results, this project has a low risk of CO_2 leakage, and well stability and existing faults are the major risk factors in the short term. However, reservoir permeability and porosity take turns in dominating the leakage risk over the long term (e.g., 30 years). The eastern part of the study area was classified as a leakage-prone area due to the existence of high-permeability strata. Because the CO_2 leakage risk and critical risk factors dynamically change with time, a monitoring program needs to be dynamically deployed in conjunction with different time periods.

This study innovatively combined numerical simulation results with quantitative evaluation scoring indices, realizing directional feature application of the evaluation method. It also investigated dynamic relationships between the distribution of the CO_2 plume and the amount of leakage over a longer time scale. However, there is still a need for more accurate and specific descriptions of the leakage paths, such as the wellbore and faults, etc. The established method of cumulative multiplication of comprehensive indexes cannot accurately reflect the weight influence of each index on the overall leakage risk. In the future, more attention should also be paid to the deformation mechanism of fractures during the sealing process in the evaluation system.

Author Contributions: Writing—original draft, J.X.; Methodology, Formal analysis, Writing—review and editing, C.W.; Data curation, Visualization, D.L. (Dong Lin); Validation, X.W.; Writing—review and editing, Z.Z.; Writing—review and editing, Funding acquisition, Supervision, D.L. (Danqing Liu). All authors have read and agreed to the published version of the manuscript.

Funding: This research received no external funding.

Data Availability Statement: The data presented in this study are available on request from the corresponding author due to privacy.

Conflicts of Interest: Authors Jingwen Xiao, Dong Lin and Xiao Wu were employed by the PetroChina Southwest Oil & Gas Field Company. The remaining authors declare that the research was conducted in the absence of any commercial or financial relationships that could be construed as a potential conflict of interest.

Abbreviations

The following abbreviations are used in this manuscript:

CCUS	CO_2 capture, geological storage and utilization
EGR	Enhanced Gas Recovery
CASSIF	Containment Assurance Scenario and Significance Identification Framework
FEP	Features, Events, and Processes
SWIFT	Structured What-If Technique
VEF	Vulnerability Evaluation Framework
P&R	Performance and Risk
CFA	Certification Framework Approach
CO_2-PENS	CO_2-Predicting Engineered Natural Systems
RISCS	Risk Interference Subsurface CO_2 Storage

PRA	Probabilistic Risk Assessment Method
FTA	Fault Tree Analysis

References

1. Huang, W.; Xiao, Y.; Li, X.; Ning, Z. Leakage diffusion and safety assessment of CO_2 pipeline transportation flange based on CFD simulation. *Greenh. Gases* **2024**, *14*, 728–742. [CrossRef]
2. Nath, F.; Mahmood, M.N.; Yousuf, N. Recent advances in CCUS: A critical review on technologies, regulatory aspects and economics. *Geoenergy Sci. Eng.* **2024**, *238*, 212726. [CrossRef]
3. Chen, S.; Liu, J.; Zhang, Q.; Teng, F.; McLellan, B.C. A critical review on deployment planning and risk analysis of carbon capture, utilization, and storage (CCUS) toward carbon neutrality. *Renew. Sustain. Energy Rev.* **2022**, *167*, 112537. [CrossRef]
4. Ahmed, S.; Khan, M.K.; Kim, J. Revolutionary advancements in carbon dioxide valorization via metal-organic framework-based strategies. *Carbon. Capture Sci. Technol.* **2025**, *15*, 100405. [CrossRef]
5. Su, X.; Liu, S.; Zhang, L.; Liu, G.; Wang, Y.; Gan, M.; Li, X. Wellbore leakage risk management in CO_2 geological utilization and storage: A review. *Energy Rev.* **2023**, *2*, 100049. [CrossRef]
6. Lv, H.; Wang, L.; Liu, G.; Lou, Z.; Pang, L.; Cai, B.; Li, Q. Risk assessment on the CCUS project using risk breakdown structure methodology: A case study on Jilin oilfield CO_2-EOR Hei-79 block. *Greenh. Gases* **2021**, *11*, 750–763. [CrossRef]
7. Wang, F.; Cao, J.; Zhang, Y.; Aviso, K.B.; Tan, R.R.; Li, Z.; Jia, X. Safety risk assessment of the large-scale carbon capture, utilization, and storage demonstration project in Dongying, China. *J. Clean. Prod.* **2023**, *414*, 137699. [CrossRef]
8. Rui, Z.; Zeng, L.; Dindoruk, B. Challenges in the Large-Scale Deployment of CCUS. *Engineering* **2025**, *44*, 17–20. [CrossRef]
9. Wang, Z.; Li, H.; Liu, S.; Xu, J.; Liu, J.; Wang, X. Risk evaluation of CO_2 leakage through fracture zone in geological storage reservoir. *Fuel* **2023**, *342*, 127896. [CrossRef]
10. Yavuz, F.; van Tilburg, T.; David, P.; Spruijt, M.; Wildenborg, T. Second Generation CO_2 FEP Analysis: CASSIF—Carbon Storage Scenario Identification Framework. *Energy Procedia* **2009**, *1*, 2479–2485. [CrossRef]
11. Condor, J.; Unatrakarn, D.; Wilson, M.; Asghari, K. A comparative analysis of risk assessment methodologies for the geologic storage of carbon dioxide. *Energy Procedia* **2011**, *4*, 4036–4043. [CrossRef]
12. EPA, U. *Vulnerability Evaluation Framework for Geologic Sequestration of Carbon Dioxide*; Epa 430-R-08-009; U.S. Environmental Protection Agency: Washington, DC, USA, 2008.
13. Barros, E.G.D.; Leeuwenburgh, O.; Szklarz, S.P. Quantitative assessment of monitoring strategies for conformance verification of CO_2 storage projects. *Int. J. Greenh. Gas. Con.* **2021**, *110*, 103403. [CrossRef]
14. Sneddon, J.; Busby, A.; Hurst, S. Practical Qualitative and Quantitative Models in Carbon Capture Utilization and Storage Risk Assessment. In Proceedings of the Offshore Technology Conference, Houston, TX, USA, 6–9 May 2024; p. D031S042R002.
15. Le Guen, Y.; Le Gouevec, J.; Chammas, R.; Gerard, B.; Poupard, O.; Van Der Beken, A.; Jammes, L. CO_2 Storage: Managing the Risk Associated With Well Leakage Over Long Time Scales. *SPE Proj. Facil. Constr.* **2009**, *4*, 87–96. [CrossRef]
16. Oldenburg, C.M. Screening and ranking framework for geologic CO_2 storage site selection on the basis of health, safety, and environmental risk. *Environ. Geol.* **2008**, *54*, 1687–1694. [CrossRef]
17. Stauffer, P.H.; Pawar, R.J.; Surdam, R.C.; Jiao, Z.; Deng, H.; Lettelier, B.C.; Viswanathan, H.S.; Sanzo, D.L.; Keating, G.N. Application of the CO_2-PENS risk analysis tool to the Rock Springs Uplift, Wyoming. *Energy Procedia* **2011**, *4*, 4084–4091. [CrossRef]
18. Bielicki, J.M.; Pollak, M.F.; Wilson, E.J.; Fitts, J.P.; Peters, C.A. A Methodology for Monetizing Basin-Scale Leakage Risk and Stakeholder Impacts. *Energy Procedia* **2013**, *37*, 4665–4672. [CrossRef]
19. Junji Yamaguchi, A.; Sato, T.; Tobase, T.; Wei, X.; Huang, L.; Zhang, J.; Bian, J.; Liu, T. Multiscale numerical simulation of CO_2 hydrate storage using machine learning. *Fuel* **2023**, *334*, 126678. [CrossRef]
20. Sori, A.; Moghaddas, J.; Abedpour, H. Comprehensive review of experimental studies, numerical modeling, leakage risk assessment, monitoring, and control in geological storage of carbon dioxide: Implications for effective CO_2 deployment strategies. *Greenh. Gases* **2024**, *14*, 887–913. [CrossRef]
21. Lu, S.; Jiang, P.; Cong, L.; Lü, X. Research Progress on CO_2 Geological Storage Reservoir and Caprock Mechanics: Methods and Status. *Greenh. Gases* **2025**, *15*, 264–276. [CrossRef]
22. Gao, S.; Jia, S.; Zhu, Y.; Zhao, L.; Cao, Y.; Qi, X.; Guan, F. Study on Quantitative Assessment of CO_2 Leakage Risk Along the Wellbore Under the Geological Storage of the Salt Water Layer. *Energies* **2024**, *17*, 5302. [CrossRef]
23. Sorgi, C.; De Gennaro, V.; Mandiuc, A. A New Methodology for Quantitative Risk Assessment of CO_2 Leakage in CCS Projects. *Spe. J.* **2024**, *29*, 7214–7233. [CrossRef]
24. Dou, N.; Hu, Z.; Wang, Z.; He, H.; Yang, S. Risk Assessment of Annular Pressure Caused by Tubing Leakage in Offshore Gas Wells with High CO_2. *Geofluids* **2023**, *2023*, 9072217. [CrossRef]
25. Hajiyev, E.; Watson, M.; Emadi, H.; Eissa, B.; Hussain, A.; Baig, A.R.; Shahin, A. A Comparative Study of Major Risk Assessment (RA) Frameworks in Geologic Carbon Storage (GCS). *Fuels* **2025**, *6*, 42. [CrossRef]

26. Zhang, L.; Cao, C.; Wen, S.; Zhao, Y.; Peng, X.; Wu, J. Thoughts on the development of CO_2-EGR under the background of carbon peak and carbon neutrality. *Nat. Gas. Ind. B* **2023**, *10*, 383–392. [CrossRef]
27. Li, Q.; Liu, G. Risk Assessment of the Geological Storage of CO_2: A Review. In *Geologic Carbon Sequestration: Understanding Reservoir Behavior*; Vishal, V., Singh, T.N., Eds.; Springer International Publishing: Cham, Switzerland, 2016; pp. 249–284.
28. Zhang, Y.; Oldenburg, C.M.; Benson, S.M. Vadose Zone Remediation of Carbon Dioxide Leakage from Geologic Carbon Dioxide Sequestration Sites. *Vadose Zone J.* **2004**, *3*, 858–866. [CrossRef]
29. Gholami, R.; Raza, A.; Iglauer, S. Leakage risk assessment of a CO_2 storage site: A review. *Earth-Sci. Rev.* **2021**, *223*, 103849. [CrossRef]
30. Jing, M.; Li, Q.; Liu, G.; Xue, Q. Quantitative assessment of CO_2 leakage risk in geologic carbon storage management. *Greenh. Gases* **2024**, *14*, 1068–1091. [CrossRef]
31. Jia, R.; Fu, X.; Jin, Y.; Wu, T.; Wang, S.; Cheng, H. Mechanical properties of mudstone caprock and influencing factors: Implications for evaluation of caprock integrity. *Front. Earth Sci.* **2023**, *11*, 1229851. [CrossRef]
32. Xiao, T.; Xu, H.; Moodie, N.; Esser, R.; Jia, W.; Zheng, L.; Rutqvist, J.; McPherson, B. Chemical-Mechanical Impacts of CO_2 Intrusion Into Heterogeneous Caprock. *Water Resour. Res.* **2020**, *56*, e2020WR027193. [CrossRef]
33. Watson, T.L.; Bachu, S. Identification of Wells with High CO_2-Leakage Potential in Mature Oil Fields Developed for CO_2-Enhanced Oil Recovery. In Proceedings of the SPE Symposium on Improved Oil Recovery, Tulsa, OK, USA, 20–23 April 2008; p. SPE-112924-MS.
34. Lackey, G.; Vasylkivska, V.S.; Huerta, N.J.; King, S.; Dilmore, R.M. Managing well leakage risks at a geologic carbon storage site with many wells. *Int. J. Greenh. Gas. Con.* **2019**, *88*, 182–194. [CrossRef]
35. Lu, J.; Lv, Y.; Fang, X.; Zuo, J.; Wang, S.; Li, H.; Yuan, C.; Liu, W. Fault Leakage Behaviors and Co_2 Migration in Different Types of Geological Carbon Storage. *Chem. Technol. Fuels Oils* **2024**, *60*, 471–480. [CrossRef]
36. Fu, X.; Jia, R.; Wang, H.; Wu, T.; Meng, L.; Sun, Y. Quantitative evaluation of fault-caprock sealing capacity: A case from Dabei-Kelasu structural belt in Kuqa Depression, Tarim Basin, NW China. *Pet. Explor. Dev.* **2015**, *42*, 329–338. [CrossRef]
37. Xu, J.; Zhou, Y.; Pan, R.; Huang, T.; Liu, B.; Gao, Q.; Liu, Y. The Integrity Evaluation of Geological Body for CCUS Technology Based on Microseismic Monitoring Technology. In Proceedings of the ADIPEC, Abu Dhabi, United Arab Emirates, 4–7 November 2024; p. D021S061R004.
38. Eaton, B.A. Fracture Gradient Prediction and Its Application in Oilfield Operations. *J. Pet. Technol.* **1969**, *21*, 1353–1360. [CrossRef]
39. Liu, D.; Agarwal, R.; Liu, F.; Yang, S.; Li, Y. Modeling and assessment of CO_2 geological storage in the Eastern Deccan Basalt of India. *Environ. Sci. Pollut. Res.* **2022**, *29*, 85465–85481. [CrossRef]

Disclaimer/Publisher's Note: The statements, opinions and data contained in all publications are solely those of the individual author(s) and contributor(s) and not of MDPI and/or the editor(s). MDPI and/or the editor(s) disclaim responsibility for any injury to people or property resulting from any ideas, methods, instructions or products referred to in the content.